PAPER

Check for updates

Surfactant-coated iron oxide nanoparticles synthesized by coprecipitation as potential phosphate adsorbents in peritoneal dialysis

Théo Lucante,[ab] Anne Carton,[a] Jan Niklas Schmidt, [ID][a] Céline Kiefer,[a] Philippe Choquet,[cde] Ariane Zaloszyc[bef] and Sylvie Bégin-Colin [ID] *[ab]

Iron oxide nanoparticles (IONPs) were recently shown to be effective phosphate adsorbents for enhancing phosphate removal during peritoneal dialysis (PD) treatment. However, such application requires surfactant-coated IONPs synthesized using a sustainable and easy scalable synthesis method displaying a high specific surface area for ensuring a high phosphate removal and a high colloidal stability in dialysate used for PD (exhibiting a high osmolarity and ionic strength). To address these challenges, we have developed the synthesis by the coprecipitation method of IONPs coated with three different surfactants: polyacrylic acid (PAA), tannic acid (TA), and polydiallyldimethylammonium chloride (PDADMAC). Stable colloidal suspensions of PAA- and TA-coated IONPs in pH 7 water and dialysate were obtained by performing the coprecipitation in the presence of surfactants, while stable suspensions of PDADMAC-coated IONPs were manufactured by a two-step process. PAA- and TA-coated IONP suspensions exhibited a lower mean hydrodynamic size compared to PDADMAC-coated IONP suspensions. They all showed a high long-term colloidal stability in dialysate: at least 3 weeks for PAA- and TA-coated IONP suspensions and one week for PDADMAC-coated IONP suspensions. Furthermore, they were demonstrated to be more colloidally stable in dialysate than commercial maghemite nanoparticles coated with similar surfactants. Phosphate adsorption studies evidenced the high phosphate removal capacities of PDADMAC- and PAA-coated IONPs compared to TA-coated ones, which were removed as potential adsorbents due to the formation of a TA-phosphate complex. Thus, this study highlights PDADMAC- and PAA-coated IONPs as promising phosphate adsorbents to be further tested under PD simulating conditions.

1 Introduction

Spinel iron oxide nanoparticles (IONPs) have been widely developed due to their broad range of applications in numerous domains: nanomedicine,[1–3] data storage,[4] catalysis,[5] *etc*. In particular, IONPs are biocompatible and biodegradable and have a low toxicity,[6,7] which has enabled their extensive development for biomedical applications: as contrast agents for magnetic resonance imaging;[8–11] as therapeutic agents through magnetic hyperthermia and photothermia,[12–17] as oral phosphate binders,[18] *etc*. However, the use of naked IONPs for applications requiring a high colloidal stability in aqueous media is limited by their isoelectric point (IEP) located at $pH_{IEP} \approx 7$.[19] At pH_{IEP}, the zeta potential (ζ) value of IONPs is overall zero, lowering electrostatic repulsions between them and greatly reducing their colloidal stability. To overcome this, a widely used strategy is to coat IONPs with surfactants, *i.e.* compounds (molecules, polymers, *etc.*) that can adsorb chemically (through anchoring groups) and/or physically (*e.g.*, electrostatically) onto the surface of IONPs, favoring electrostatic and/or steric repulsive forces between nanoparticles.[19–22] Furthermore, biomedical applications notably require IONPs with a high colloidal stability in media with high osmolarity and ionic strength. Indeed, media such as blood plasma[23,24] or dialysate[25,26] used in peritoneal dialysis (Table S1), contain various solutes and electrolytes (proteins, glucose, mineral ions, *etc.*) that can significantly alter the nanoparticle colloidal stability. For example, a well-known effect is the "charge-screening effect" generated by electrolytes: the counter-ions

[a]University of Strasbourg and CNRS, Institut de Physique et Chimie des Matériaux de Strasbourg, UMR 7504, 23 Rue Du Loess, 67034 Strasbourg Cedex 2, France. E-mail: sylvie.begin@unistra.fr

[b]University of Strasbourg and CNRS, Institut de Chimie et Procédés pour l'Énergie, L'Environnement et la Santé, UMR 7515, 25 Rue Becquerel, 67087 Strasbourg, France

[c]University of Strasbourg and CNRS, Laboratoire des Sciences de l'Ingénieur, de L'Informatique et de l'Imagerie, UMR 7357, France

[d]Preclinical Imaging Lab, Imaging Dpt, Hôpitaux Universitaires de Strasbourg, Strasbourg, France

[e]University of Strasbourg, Faculté de Médecine, Maïeutique et Sciences de la Santé, Strasbourg, France

[f]Nephro-pediatry, CHU Hautepierre, Hopitaux Universitaire de Strasbourg, 1 Avenue Molière, 67098 Strasbourg, France

could organize around the charged surfactant-coated nanoparticles, decreasing their Debye–Hückel screening length (*i.e.* the distance from a nanoparticle where the electrostatic force is significantly reduced)[27] and thus the intensity of the electrostatic repulsion between them, leading to the destabilization of the nanoparticle suspension.

In particular, we are looking, in this work, for stable suspensions of surfactant-coated IONPs in a dialysate suspension used in the peritoneal dialysis (PD) process. PD is a medical treatment for people suffering from end-stage renal disease (ESRD) during which the dialysate (typically ≈ 2 liters) is infused into the patient's peritoneal cavity.[25,26] There, compounds and toxins in chronic excess in the blood of ESRD patients are transported to the dialysate through the peritoneal membrane – a biological membrane layering the peritoneal cavity.[28] The formulation of dialysate, which is an aqueous solution at pH $= 7.4 \pm 0.1$ containing glucose and electrolytes (Ca^{2+}, Na^+, Mg^{2+}, Cl^-, and HCO_3^-, Table S1) conferring a high osmolarity (≈ 358 mOsm L^{-1}) and ionic strength (≈ 141 mmol L^{-1}) to this solution, drove the toxin transport. Among dangerous compounds are phosphates whose clearance is currently too slow and low in a PD process when they are in excess.[25,26] In this context, the objective is to add IONPs—known for their ability to adsorb phosphates—to the composition of an existing dialysate so that they adsorb phosphates, diffusing from blood through the peritoneal membrane into the dialysate, and thus induce the diffusive transport of additional phosphates from the blood into the dialysate. From a practical point of view, the proposed methodology involves obtaining colloidally stable IONPs directly into the dialysate prior to its intraperitoneal administration. After a PD cycle, the dialysate containing uremic toxins and phosphate-loaded IONPs is extracted. Magnetic separation can then be used to remove IONPs from the dialysate. One of the major advantages of this application in terms of biosafety is that IONPs remain in the peritoneal cavity, and their high colloidal stability in the dialysate would prevent them from entering the bloodstream. In addition, the *in vivo* residence time is restricted to the duration of a standard PD cycle (approximately 4 hours). Compared to other clinical applications involving IONPs, such as MRI, such limited exposure and their localization in the dialysate should minimize toxicity risks. However, *in vitro* experiments and *in vivo* experiments will be needed to further validate this strategy.

We demonstrated recently that tannic acid-coated iron oxide nanostructures are promising phosphate adsorbents that can be introduced into the dialysate to improve phosphate removal from blood during a PD cycle.[25,26] However, these nanostructures suffer from a low long-term colloidal stability in dialysate which needs to be improved by preserving a high phosphate adsorption performance. Thus, such designed surfactant-coated IONPs must be colloidally stable for at least one day and preferably for a longer period of time so that they can be stored directly in a dialysate bag. Furthermore, they must be synthesized by a method leading to large quantities as the dialysate volume is about 2 liters and

thus an easy-scalable and, if possible, a green synthesis method should be favored.

Therefore, we focus, in this work, on the synthesis of three surfactant-coated IONPs displaying a high colloidal stability in pH 7 water and dialysate by the coprecipitation method. Indeed, it is a "green" method performed in water and known for its high yield of IONPs.[29–31] The selected surfactants are polyacrylic acid (PAA), tannic acid (TA) and polydiallyldimethylammonium chloride (PDADMAC). PAA and TA are anionic surfactants approved by the Food and Drug Administration (FDA) as food additives[32,33] and are known to anchor to the iron oxide (IO) surface through their carboxylate and catechol groups respectively.[22] Indeed, PAA is reported to be an effective surfactant for IONPs by forming surface complexes (unidentate, bidentate and bridging complexes[19,22]) through interactions between its multiple carboxylate groups and IONP hydroxyl surface groups.[22,34–36] On the other hand, TA catechol units are reported to coordinate with the IO surface through orbital overlap of the five-membered ring leading to strong binding.[19] Since the pK_a values of PAA and TA are 4.3–4.5 [37–39] and ~ 6 [40] respectively, these functional groups are deprotonated at pH 7, giving a negative ζ value to the surfactant-coated IONPs, thus enhancing their colloidal stability by promoting electrostatic repulsions between them. In the literature, these two surfactants have been widely used to coat IONPs, either *in situ*[34,41–45] or prior to[46–51] the synthesis of IONPs. In parallel, PDADMAC is a polymer with a permanent cationic charge approved by the FDA for treatment of potable water.[52] It has been selected because we would like to study the influence of the "surface charge" of IONPs on phosphate adsorption, because it is widely used in the literature to coat IONPs[53–55] and has a relatively low toxicity compared to other cationic surfactants (notably polyethyleneimine).[56]

Two coating strategies have been tested either by introducing surfactants during the coprecipitation step (called "one-pot synthesis") or by coating naked IONPs with surfactants after the coprecipitation step (called "post-synthesis coating"). Post-synthesis coatings are carried out in water to retain the benefits of the "green" aspect of coprecipitation and consisted in favoring electrostatic attractions between surfactants and IONPs through pH adjustments.[57,58] A protocol for accelerating the size separation step of nanograin aggregates has been established using an external magnetic field. PAA- and TA-coated IONPs obtained by the one-pot synthesis were shown to display a high long-term colloidal stability for 3 weeks in pH 7 water and dialysate. Stable suspensions of PDADMAC-coated IONPs were also obtained by post-synthesis coating and with a mean hydrodynamic diameter higher than those of PAA- and TA-coated IONPs. PAA- and PDADMAC-coated IONPs were furthermore shown to display a higher colloidal stability in dialysate than commercial IONPs coated with the same surfactants.[59] Finally, phosphate adsorption experiments demonstrated that PAA- and PDADMAC-coated IONPs are the most suitable phosphate adsorbents to be tested in the future in PD simulating processes.
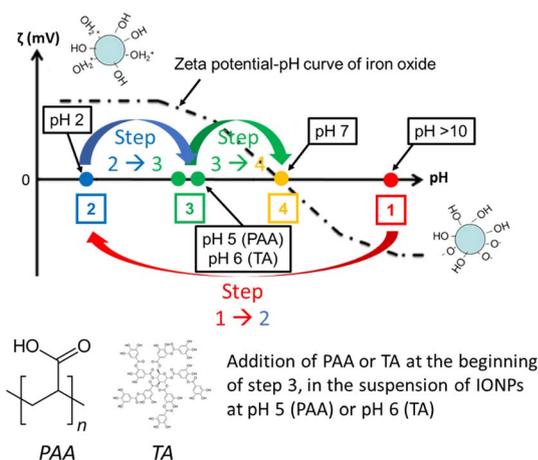
Fig. 1 Schematic of the coating protocol with PAA and TA. The dashed line represents a typical zeta potential–pH curve of naked IONPs. Step 1 → 2: quick adjustment from pH > 10 to 2 to turn the naked IONPs ζ positive. Step 2 → 3: adjustment from pH 2 to a value above surfactant pK_a (deprotonated, thus negatively charged) and below the IO IEP (naked IONPs with slightly positive ζ). Step 3 → 4: addition of the surfactant (here, PAA or TA) and then adjustment to pH 7.

2 Results and discussion

2.1 Synthesis methods of surfactant-coated IONPs

Naked IONPs are synthesized by the well-known Massart coprecipitation method[60] using the protocol of Daou et al.[30]. Two strategies have been tested to obtain surfactant-coated IONPs: the one-pot synthesis by introducing the surfactant during the coprecipitation step (@) and post-synthesis (+) coating of naked IONPs. The parameter to select the suitable synthesis protocol is the colloidal stability of surfactant-coated IONPs in both pH 7 water and dialysate.

Protocols for the post-synthesis coating of naked IONPs with surfactants have been developed based on previous

studies[57,58,61,62] by favoring electrostatic interactions between the surfactants and the charged surface of IONPs. Indeed, the IO surface possesses hydroxyl groups (Fe–OH sites) with ~20% being amphoteric.[61] At pH values below the IO IEP (pH$_{IEP}$ ≈ 7[19]), these surface groups are protonated, giving a positive ζ value to IONP suspensions. Above the IO IEP, these groups are deprotonated, giving a negative ζ value to IONP suspensions. The same strategy is used here: the coatings are performed at pH values intermediate between the IO IEP and the surfactant pK_a (PAA: pK_a = 4.3–4.5[37–39], TA: pK_a ≈ 6[40], PDADMAC: no pK_a/pK_b value and always positively charged) for favoring electrostatic attractions between them. Each post-synthesis coating is performed starting from a suspension of naked IONPs in basic pH water (pH = 9–10) with a monomodal and moderately polydisperse hydrodynamic size (φ_{hydro}) distribution, a mean φ_{hydro} value of 161 ± 86 nm and a polydispersity index (PDI) of 0.15 (Fig. S1a–c and Table S2). Zeta potential (ζ) of naked IONPs in basic pH water is −36 ± 1 mV. The performed post-coating strategy is illustrated in Fig. 1.

For the PDADMAC surfactant, the naked IONP suspension is at basic pH after coprecipitation and its pH is adjusted to 9–10 in order to favor electrostatic interactions between the negatively charged IONP surface and the positively charged PDADMAC. The so-obtained PDADMAC-coated IONPs are named IONPs+PDADMAC and their colloidal stability in pH 7 water and dialysate has been studied (Fig. 2a, b and Table 1) through dynamic light scattering (DLS) and electrophoretic light scattering (ELS). Their φ_{hydro} distribution is monomodal and moderately polydisperse in pH 7 water, with a mean φ_{hydro} value of 377 ± 159 nm and a PDI of 0.21 (Fig. 2a and Table 1). In dialysate (Fig. 2b), the φ_{hydro} distribution remains monomodal with a significant increase in mean φ_{hydro} to 544 ± 254 nm (PDI = 0.19) (Table 1). This increase in φ_{hydro} is attributed to the dialysate electrolytic composition (Table S1), especially affecting the IONPs+PDADMAC suspension even though no sedimentation is observed. The electrolyte influence has further
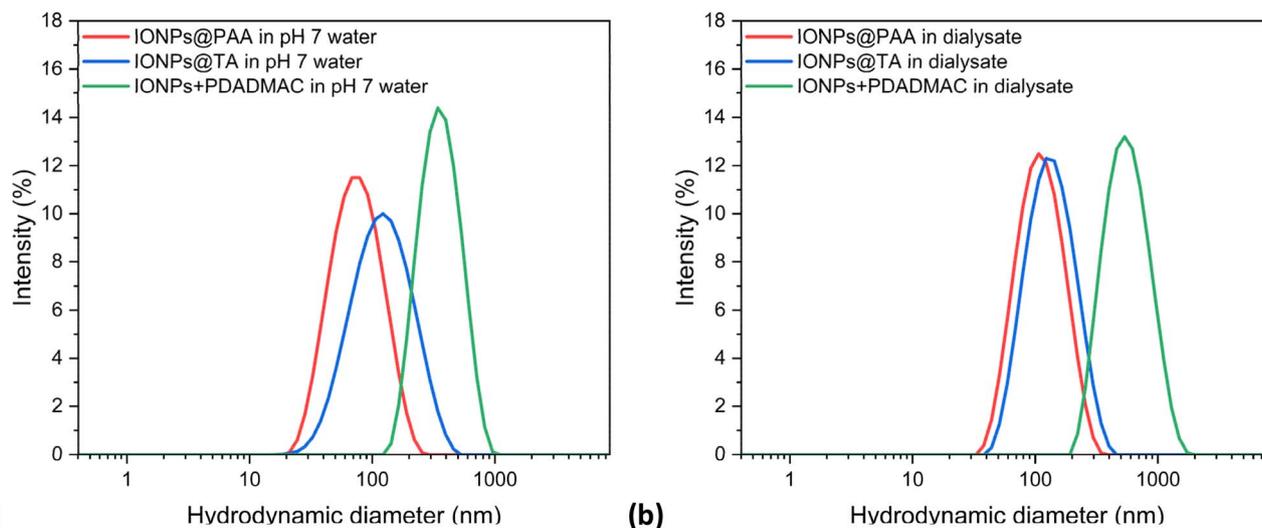

Fig. 2 Hydrodynamic diameter distributions by intensity of PAA-, TA- and PDADMAC-coated IONPs after optimization of their synthesis protocol in (a) water (pH = 7.2 ± 0.2) and (b) dialysate (pH = 7.4 ± 0.1). IONPs+PDADMAC were obtained by post-synthesis coating of naked IONPs while IONPs@PAA and IONPs@TA were obtained by the one-pot synthesis.

Table 1 Hydrodynamic diameter by intensity, mean PDI and mean zeta potential values of the surfactant-coated IONPs in pH 7 water and dialysate. IONPs+PDADMAC were obtained by post-synthesis coating of naked IONPs while IONPs@PAA and IONPs@TA were obtained by the one-pot synthesis

	φ_{hydro} by intensity (nm)		PDI		ζ (mV)	
	Water	Dialysate	Water	Dialysate	Water	Dialysate
IONPs@PAA	81 ± 36	101 ± 51	0.16	0.22	-46 ± 2	-22 ± 2
IONPs@TA	135 ± 68	150 ± 73	0.22	0.21	-38 ± 1	-23 ± 1
IONPs+PDADMAC	377 ± 159	544 ± 254	0.21	0.19	27 ± 1	20 ± 1

been investigated through ζ measurements. In pH 7 water, the mean ζ value of IONPs+PDADMAC is positive: 27 ± 1 mV (Table 1) and decreases to 20 ± 1 mV in dialysate, confirming the charge-screening effect due to electrolytes in dialysate and explaining the observed aggregation of IONPs+PDADMAC.

In the case of PAA and TA surfactants, as they are negatively charged above pH $\approx$ 4, one needs IONP suspensions with a positive surface charge thus to decrease the pH of naked IONPs below pH = 7 knowing that they may aggregate during this step. The different steps for the PAA- and TA-coating of naked IONPs are summarized in Fig. 1 and are detailed in the SI part (Section SI.I, Fig. S1a–d and Table S2). The suspension characteristics have been followed at each step of the coating protocol. The φ_{hydro} distributions of the so-obtained PAA and TA post-synthesis-coated IONPs are monomodal, with mean φ_{hydro} values of 310 ± 150 nm (PDI = 0.22, Fig. S1a) and 318 ± 186 nm (PDI = 0.23, Fig. S1b), respectively. Their ζ values are negative: -44 ± 1 mV (PAA-coated IONPs) and -36 ± 1 mV (TA-coated IONPs), suggesting successful surfactant coatings. All these results are summarized in Table S2.

However, PAA and TA post-coated IONPs undergo a significant sedimentation within 4 hours when suspended in pH 7 water. In dialysate, the sedimentation is faster (∼minutes) and complete due to the electrolyte-induced charge-screening effect. Therefore, the post-synthesis protocol does not enable the production of stable suspensions of TA and PAA post-coated IONPs in pH 7 water and dialysate. Even though their ζ values are highly negative in pH 7 water (Table S2) ensuring electrostatic repulsions between nanoparticles, their φ_{hydro} should still be too high (Table S2) limiting their long-time colloidal stability. Particularly for TA-coated IONPs, their low colloidal stability would also be due to the difficult anchoring of catechol at the IONP surface due to the high sensitivity of catechol to oxidation as a function of pH, as detailed in the SI part (Section SI.I).

The one-pot synthesis has then been tested for all surfactants. It was unsuccessful with PDADMAC despite several tests (no crystalline phase was observed to form) while stable suspensions were obtained with PAA and TA surfactants. PAA-coated IONPs are synthesized by coprecipitation using an adapted protocol from that of Daou *et al.*[30] where the surfactant is added to the mixture of iron precursors, before adding the base. With TA, as this surfactant has been demonstrated to reduce Fe(III) to Fe(II) as soon as they are mixed,[63] only Fe^{III}Cl$_3$·6H$_2$O was used as an iron precursor. Otherwise, the protocols were similar and are described in the Materials and methods part. After this one-pot synthesis, the suspensions were

observed to display a very broad hydrodynamic size distribution of particles, and an optimized size separation process has been established by comparing natural sedimentation and magnetic size separation. The optimization of the size separation process is detailed in the SI part (Section SI.II, Fig. S2a and b) and the magnetic sedimentation was shown to be very effective and reproducible, leading to suspensions with a monomodal φ_{hydro} distribution.

The so-obtained IONPs were named IONPs@TA and IONPs@PAA. Their φ_{hydro} distribution is monomodal and moderately polydisperse in pH 7 water with φ_{hydro} values of 81 ± 36 nm (PDI = 0.16) and 135 ± 68 nm (PDI = 0.22) for IONPs@PAA and IONPs@TA respectively (Table 1). In dialysate (Fig. 2b), the φ_{hydro} distributions remain monomodal with a slight increase in φ_{hydro} for IONPs@PAA and IONPs@TA: 101 ± 51 nm (PDI = 0.22) and 150 ± 73 nm (PDI = 0.21), respectively (Table 1). For each suspension in dialysate, these increases in φ_{hydro} are attributed, as for IONPs+PDADMAC, to the dialysate electrolytic composition (Table S1). This was confirmed through ζ measurements. In pH 7 water, they display a strongly negative ζ: -46 ± 2 mV (IONPs@PAA) and -38 ± 1 mV (IONPs@TA) (Table 1). All these high net values would explain the remarkable colloidal stability of each suspension in pH 7 water, where colloids repel each other through electrostatic interactions. In dialysate, the ζ values decrease to -22 ± 2 mV (IONPs@PAA) and -23 ± 1 mV (IONPs@TA) (Table 1) confirming that electrolytes in dialysate tend to destabilize each suspension by inducing a charge-screening effect.

To conclude, colloidally stable PAA- and TA-coated IONPs (IONPs@PAA and IONPs@TA respectively) are obtained by one-pot synthesis while PDADMAC-coated IONPs (IONPs+PDADMAC) are obtained by post-synthesis coating of naked IONPs.

2.2. Structural and surface characterization of surfactant-coated IONPs

Transmission electron microscopy (TEM) images of naked and surfactant-coated IONPs are presented in Fig. 3a–d. Naked IONPs consist of aggregates of nanograins (Fig. 3a), as usually observed with nanoparticles synthesized by coprecipitation. The aggregation state appears to be less "dense" when IONPs are coated with surfactants (Fig. 3b–d), supporting their presence at their surface. Naked IONPs and IONPs+PDADMAC display a similar TEM diameter, 10 ± 3 nm and 9 ± 3 nm respectively (Fig. 3e), in agreement with the post-synthesis coating of naked IONPs after coprecipitation. On the other
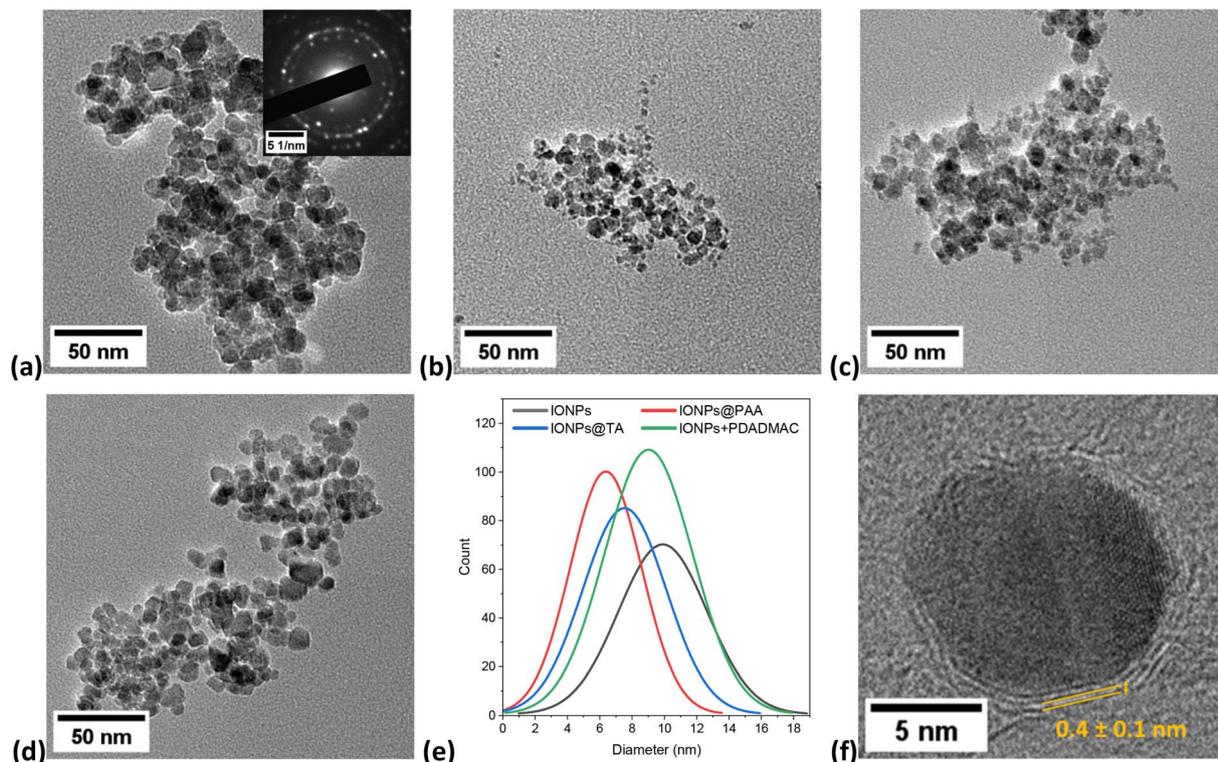
Fig. 3 TEM image of (a) naked IONPs (inset: the selected area electron diffraction (SAED) pattern of one aggregate), (b) IONPs@PAA, (c) IONPs@TA and (d) IONPs+PDADMAC. (e) TEM diameter Gaussian distribution of each nanoparticle (statistical samples of >300 nanoparticles). (f) HRTEM image of one IONP@PAA.

hand, IONPs@PAA and IONPs@TA exhibit smaller grain sizes 6 ± 2 nm and 8 ± 3 nm respectively (Fig. 3e) demonstrating the impact of the presence of the surfactant during the coprecipitation step, especially with PAA. In the case of the one-pot coprecipitation synthesis, Lin et al.[41] proposed that PAA acts as a template for IONP nucleation, inhibiting their growth while confining them in the polymer matrix. In our previous work, we also observed the ability of TA to hinder the growth of IO grains in the polyol solvothermal synthesis.[63] However, it can be noted that such a surfactant-induced size-decrease effect in one-pot coprecipitation synthesis is not systematic. Filippousi et al.[64] reported an opposite trend in the presence of the cationic surfactant cetyltrimethylammonium bromide, the non-ionic surfactant polyvinylpyrrolidone K 30 and the anionic surfactant sodium cholate.

A high-resolution TEM image of an isolated IONP@PAA (Fig. 3f) allowed observation of PAA layers at its surface. By using the "plot profile" function of the ImageJ software on the inverse Fourier transform of several areas at the nanoparticle edge, we found that this nanoparticle is coated with two PAA layers of thickness 0.4 ± 0.1 nm. However, it should be noted that IONPs@PAA are statistically found as aggregates of ∼80–100 nm in size (Table 2), with several PAA layers covering the whole aggregates.

X-ray diffraction (XRD) patterns in Fig. S3 display the characteristic XRD peaks of the IO spinel phase for each surfactant-coated IONP. The lattice parameter and crystallite size have been determined by performing a profile matching on XRD patterns using the FullProf software, and these values are reported in Table 2. The lattice parameter of each nanoparticle is estimated to be 8.37–8.38 Å, i.e. intermediate values between those of stoichiometric magnetite (8.396 Å) and maghemite (8.346 Å) phases, in agreement with the expected composition of such IONP sizes. Indeed, IONPs with a mean diameter smaller than 15 nm display often an oxidized magnetite composition.[30,65,66] The crystallite sizes of naked and PDADMAC-coated IONPs are 10 ± 3 nm and 9 ±

Table 2 Lattice parameter, crystallite size and TEM size of naked and surfactant-coated nanoparticles

	Maghemite Fe$_2$O$_3$	Magnetite Fe$_3$O$_4$	IONPs	IONPs@PAA	IONPs@TA	IONPs+PDADMAC
Lattice parameter (Å)	8.346[a]	8.396[b]	8.38 ± 0.01	8.37 ± 0.01	8.38 ± 0.01	8.38 ± 0.01
XRD crystallite size (nm)	—	—	10 ± 1	6 ± 1	6 ± 1	9 ± 1
TEM size (nm)	—	—	10 ± 3	6 ± 2	8 ± 3	9 ± 3

[a] From ICDD PDF card no. 00-039-1346. [b] From ICDD PDF card no. 04-005-4319.
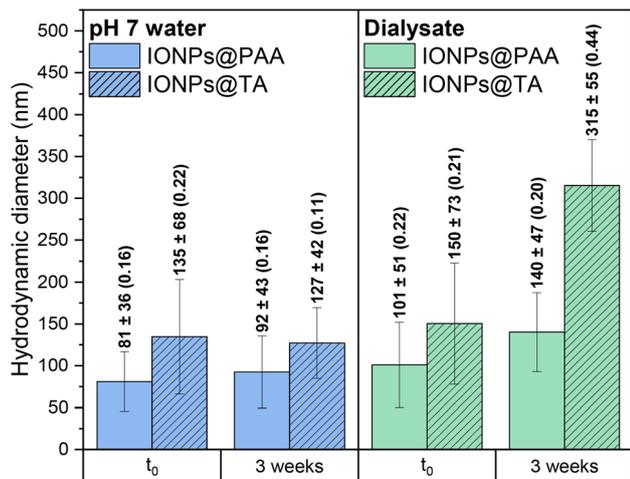
Fig. 4 Mean hydrodynamic diameter of PAA- and TA-coated IONPs at t_0 and after three weeks in pH 7 water and in dialysate.

3 nm respectively while it is 6 ± 1 nm for PAA- and TA-coated IONPs. Thus, these crystallite sizes match quite well the nanoparticle TEM diameter values (Table 2). This is in line with the SAED pattern of naked IONPs (Fig. 3a) exhibiting a typical polycrystalline structure and hence an absence of oriented aggregation in nanoparticle aggregates.[67–69]

Surfactants present on IONPs have then been characterized by Fourier-transform infrared (FTIR) spectroscopy. A broad Fe–O band is observed in Fig. S4a localized at 594 cm^{-1} (IONPs@PAA), 592 cm^{-1} (IONPs@TA) and 584 cm^{-1} (IONPs+PDADMAC). These values and the broad shoulder of this Fe–O band towards the high wavenumbers are characteristic of an oxidized magnetite phase.[63,65,70] Indeed, the IR spectrum of non-oxidized magnetite displays one Fe–O band at $\sim$580 cm^{-1} while that of maghemite exhibits several bands in the wavenumber range 800–400 cm^{-1} whose resolution depends on the ordering of vacancies in maghemite.[65] The IR spectra also show the presence of some IR bands of surfactants and the analysis of IR spectra is detailed in the SI part (Section SI.III, Fig. S4a–d and Table S3). A proposal of FTIR band attribution in surfactant-coated IONP spectra is given in Table S3. This FTIR analysis has shown that, due to the presence of a lot of carboxylates in PAA, it is difficult to identify which carboxylate complex is formed on the IO surface. The IONPs@TA spectrum (Fig. S4c) confirms the presence of TA at the surface of IONPs and the presence of IR bands attributed to a complex formed by TA on the iron oxide surface.[63] Finally, the FTIR spectrum of

IONPs+PDADMAC in Fig. S4d provided slight evidence of the surfactant presence and did not enable us to confirm the presence of the cationic surfactant, suggesting a purely physical adsorption of PDADMAC on the IO surface.

Thermogravimetric analysis (TGA) in air has been performed to confirm the presence of surfactants and quantify their amount on each type of nanoparticle. The TGA curves are given in Fig. S5 and described in the SI part (Section SI.IV). TGA curves display thermal events in accordance with that observed in the literature for these surfactants or surfactant-coated IONPs. A weight loss at 800 °C attributed to surfactants was noticed for all surfactant coated IONPs: $\sim$49% for IONPs@PAA, 58% for IONPs@TA and 66% for IONPs+PDADMAC.

2.3 Long-term colloidal stability of our surfactant-coated IONPs and comparison with commercial surfactant-coated IONPs

The long-term colloidal stability of our different surfactant-coated IONPs has been evaluated in pH 7 water and dialysate up to 3 weeks (Fig. 4). IONPs+PDADMAC do not appear in Fig. 4 because the suspensions underwent sedimentation after $\approx$1 week in pH 7 water and in dialysate. However, this duration would be sufficient for their use in PD treatment. The φ_{hydro} distribution curves of IONPs@PAA and IONPs@TA are displayed in Fig. S6a–d, and they are all monomodal.

In pH 7 water, the mean φ_{hydro} and PDI of IONPs@PAA and IONPs@TA do not increase significantly after 3 weeks, from 81 ± 36 nm (PDI = 0.16) to 92 ± 43 (PDI = 0.16) and from 135 ± 68 (PDI = 0.22) to 127 ± 42 (PDI = 0.11) respectively. Then, in dialysate, IONPs@PAA have retained a high colloidal stability over time with a slight φ_{hydro} increase from 101 ± 51 nm (PDI = 0.22) to 140 ± 47 (PDI = 0.23). However, more significant increases of IONPs@TA φ_{hydro} and PDI are observed after three weeks: from 150 ± 73 nm (PDI = 0.21) to 315 ± 55 nm (PDI = 0.44). This PDI value is relatively high because nanoparticle sedimentation occurred during measurements in triplicate with mean φ_{hydro} values in the range of 213–415 nm. Thus, the presence of glucose and electrolytes has considerably altered the TA-coated IONP colloidal stability by contrast to that of PAA-coated IONPs. Therefore, IONPs@TA are able to retain a high colloidal stability in pH 7 water up to 3 weeks and, to a lower extent, in dialysate, while IONPs@PAA display a high colloidal stability in each medium up to 3 weeks.

Then, colloidal stability over 4 hours in pH 7 water and dialysate of IONPs@PAA and IONPs+PDADMAC has been compared with that of commercial PAA- and PDADMAC-coated maghemite

Table 3 Hydrodynamic diameter by intensity, polydispersity index and zeta potential values of our own and commercial PAA- and PDADMAC-coated IONPs in pH 7 water and dialysate

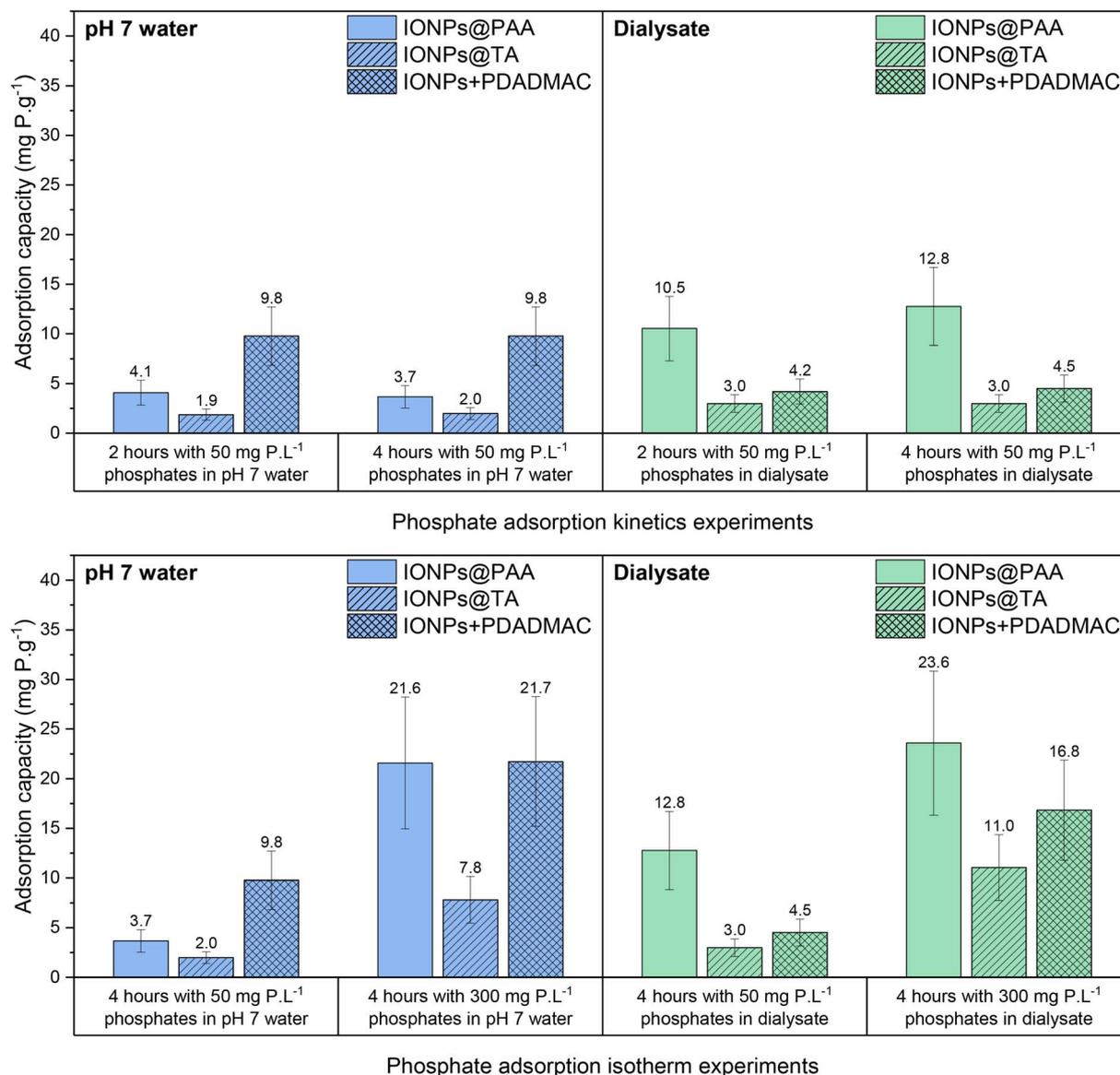|	pH 7 water			Dialysate		
	φ_{hydro} (nm)	PDI	ζ (mV)	φ_{hydro} (nm)	PDI	ζ (mV)
fluidMAG-PAA	106 ± 46	0.14	-35 ± 3	2146 ± 775	0.25	-21 ± 1
IONPs@PAA	81 ± 36	0.16	-46 ± 2	101 ± 51	0.22	-22 ± 2
fluidMAG-Q	195 ± 109	0.16	33 ± 1	1459 ± 426	0.17	9 ± 1
IONPs+PDADMAC	377 ± 159	0.21	27 ± 1	544 ± 254	0.19	20 ± 1

Fig. 5 Phosphate adsorption kinetics (top) and isotherm (bottom) experiments with surfactant-coated IONPs in pH 7 water (left) and dialysate (right). Kinetics experiments: 1 mg mL^{-1} surfactant-coated IONPs with 50 mg P L^{-1} phosphates in pH 7 water and dialysate for 2 hours and 4 hours. Isotherm experiments: 1 mg mL^{-1} surfactant-coated IONPs with 50 mg P L^{-1} and 300 mg P L^{-1} phosphates in pH 7 water and dialysate for 4 hours. All experiments are performed at room temperature.

nanoparticles named "fluidMAG-PAA" (PAA-coated IONPs, approximate φ_{hydro} provided by the supplier: 100 nm) and "fluid-MAG-Q" (PDADMAC-coated IONPs, approximate φ_{hydro} provided by the supplier: 200 nm). From TEM images (Fig. S7a and b), the commercial IONP TEM sizes are 12 ± 3 nm (fluidMAG-PAA) and 13 ± 4 nm (fluidMAG-Q) (Fig. S7c), while our IONP TEM sizes are smaller: 6 ± 2 nm (IONPs@PAA) and 9 ± 3 nm (IONPs+PDADMAC) (Table 2). The φ_{hydro} distributions of commercial IONPs in pH 7 water are monomodal with φ_{hydro} values of 106 ± 46 nm (PDI = 0.14) for fluidMAG-PAA (Fig. S8a) and 195 ± 109 nm (PDI = 0.16) for fluidMAG-Q (Fig. S8b). Their ζ values are −35 ± 3 mV (fluidMAG-PAA) and 33 ± 1 mV (fluidMAG-Q), similarly to our IONPs@PAA and IONPs+PDADMAC (Table 3). However, in dialysate, each commercial suspension is immediately destabilized: their φ_{hydro} distribution remains monomodal but their mean φ_{hydro} values largely increase to 2146 ± 775 nm, PDI = 0.25 (fluidMAG-PAA, Fig. S8a) and 1459 ± 426 nm, PDI = 0.17 (fluidMAG-Q, Fig. S8b). In addition, these suspensions undergo complete sedimentation after ~20 minutes. Furthermore, ζ measurements confirm that these destabilizations are again attributed to the charge-screening effect induced by electrolytes in dialysate: the commercial IONP net ζ values decrease to −21 ± 1 mV (fluidMAG-PAA) and 9 ± 1 mV (fluidMAG-Q). Therefore, our IONPs@PAA and IONPs+PDADMAC, displaying lower mean grain size, are less destabilized by electrolytes in dialysate compared to commercial PAA- and PDADMAC-coated maghemite nanoparticles, asserting their high potential for our application.

2.4 Phosphate adsorption on surfactant-coated IONPs in pH 7 water and dialysate

All surfactant-coated IONPs have been involved in phosphate adsorption kinetics and isotherm experiments to determine if they could rapidly adsorb a high quantity of phosphates.

Kinetic experiments, presented in the top row in Fig. 5, showed that similarly to the TA-coated iron oxide nanoclusters in our previous work,[25] the maximum adsorption capacity of each surfactant-coated IONP and whatever the media (water or dialysate) is reached in 2 hours. The phosphate adsorption values are 4.1 ± 1.3 mg P g^{-1} for IONPs@PAA, 1.9 ± 0.6 mg P g^{-1} for IONPs@TA and 9.8 ± 2.9 mg P g^{-1} for IONPs+PDADMAC in pH 7 water, compared to 10.5 ± 3.2 mg P g^{-1} for IONPs@PAA, 3.0 ± 0.9 mg P g^{-1} for IONPs@TA and 4.2 ± 1.3 mg P g^{-1} for IONPs+PDADMAC in dialysate. These values do not change significantly after 4 hours, confirming the rapid adsorption of phosphates onto surfactant-coated IONPs in each medium. In pH 7 water (top left in Fig. 5), the adsorption capacity of IONPs+PDADMAC is significantly higher than that of IONPs@PAA and IONPs@TA, certainly due to favorable electrostatic interactions. In dialysate (top right in Fig. 5), the highest adsorption capacity is no longer held by positively charged IONPs+PDADMAC but by negatively charged IONPs@PAA. Indeed, adsorption capacity of IONPs+PDADMAC decreases from 9.8 ± 2.9 mg P g^{-1} in pH 7 water to 4.2 ± 1.3 mg P g^{-1} in dialysate while that of IONPs@PAA increases

from 4.1 ± 1.3 mg P g^{-1} in pH 7 water to 10.5 ± 3.2 mg P g^{-1} in dialysate. In each medium, IONPs@TA display the lowest adsorption capacity among the three adsorbents tested and do not differ significantly in pH 7 water and in dialysate.

The adsorption isotherm experiments are presented in the bottom row in Fig. 5 and in each medium, the adsorption capacity increases with phosphate concentration. In pH 7 water (bottom left in Fig. 5), adsorption capacity increases from 3.7 ± 1.1 mg P g^{-1} to 21.6 ± 6.6 mg P g^{-1} for IONPs@PAA, from 2.0 ± 0.6 mg P g^{-1} to 7.8 ± 2.3 mg P g^{-1} for IONPs@TA and from 9.8 ± 2.9 mg P g^{-1} to 21.7 ± 6.5 mg P g^{-1} for IONPs+PDADMAC. In dialysate (bottom right in Fig. 5), adsorption capacity increases from 12.8 ± 3.9 mg P g^{-1} to 23.6 ± 7.3 mg P g^{-1} for IONPs@PAA, from 3.0 ± 0.9 mg P g^{-1} to 11.0 ± 3.3 mg P g^{-1} for IONPs@TA and from 4.5 ± 1.4 mg P g^{-1} to 16.8 ± 5.1 mg P g^{-1} for IONPs+PDADMAC. Similar to the kinetic experiments, the adsorption capacity of IONPs@PAA is the highest in dialysate for all phosphate concentrations. However, in pH 7 water, when a phosphate concentration of 300 mg P L^{-1} is used, the adsorption capacities of IONPs+PDADMAC and IONPs@PAA become very close. The adsorption capacity of IONPs@TA remains the lowest in each medium among all the nanoparticles tested and, furthermore, IONPs@TA undergo rapid and visible sedimentation in dialysate in the presence of phosphates. This sedimentation explains their lower phosphate adsorption capacity compared to IONPs@PAA and
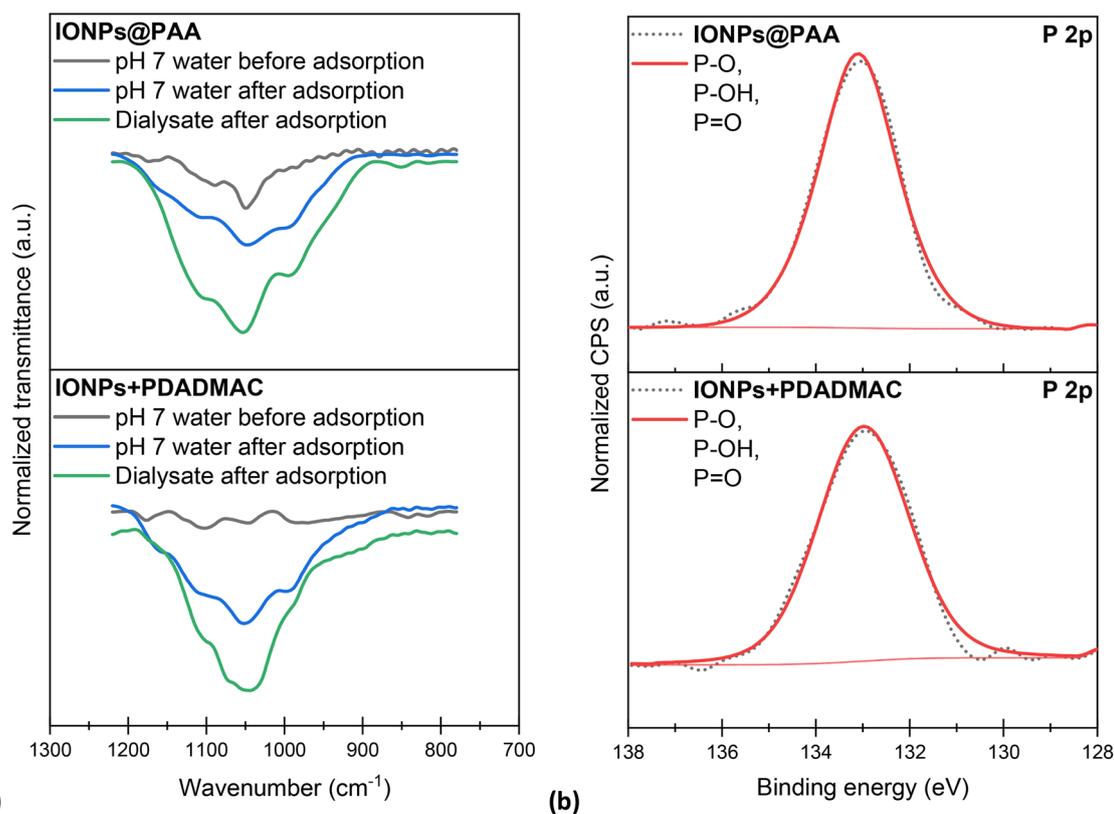

Fig. 6 (a) FTIR spectra of IONPs@PAA and IONPs+PDADMAC before and after phosphate adsorption in pH 7 water and dialysate (4 hours of contact with 300 mg P L^{-1} phosphates). (b) P 2p peak in the XPS spectra of IONPs@PAA and IONPs+PDADMAC after phosphate adsorption in pH 7 water (4 hours of contact with 300 mg P L^{-1} phosphates).
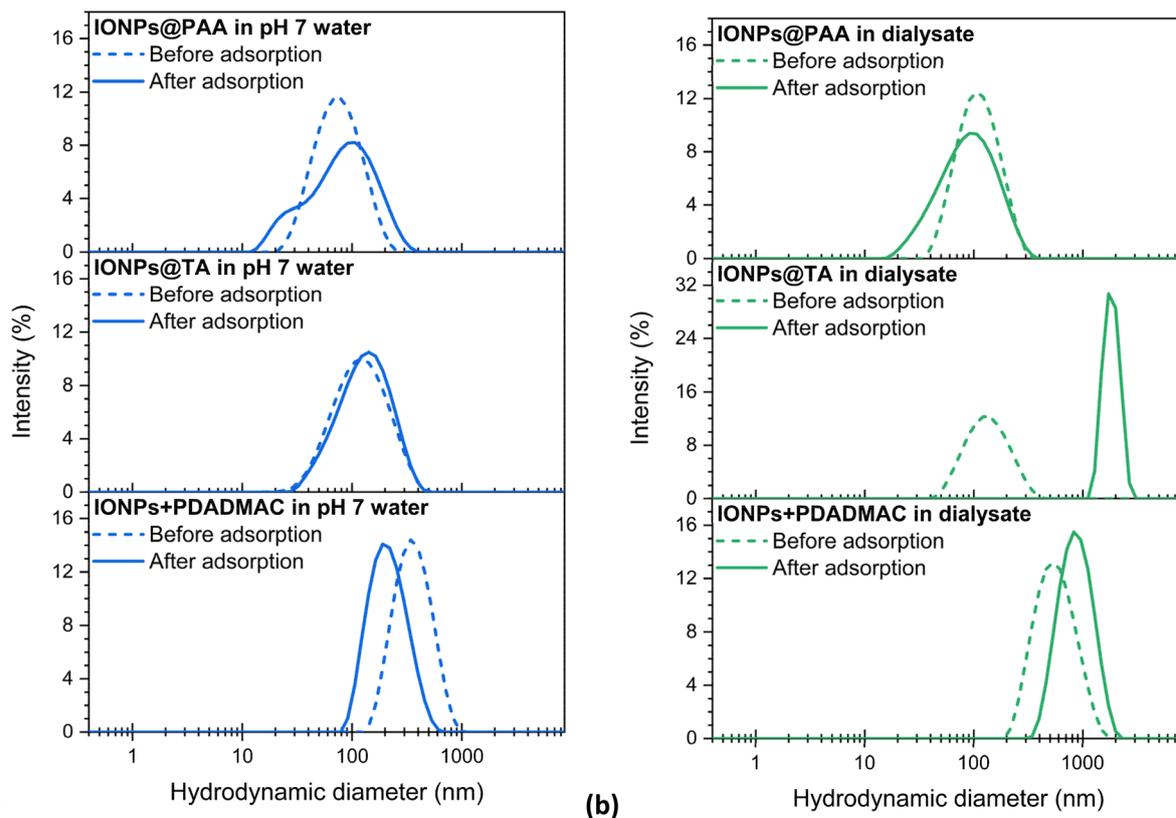
Fig. 7 Hydrodynamic diameter distributions of the different surfactant-coated IONPs before and after phosphate adsorption in (a) pH 7 water and (b) dialysate (4 hours of contact with 300 mg P L^{-1} phosphates).

IONPs+PDADMAC and leads to the exclusion of IONPs@TA for use as phosphate adsorbents in our future dialysis experiments.

We notice that the adsorption capacity values of IONPs@PAA and IONPs+PDADMAC in pH 7 water and in dialysate are close to those of TA-coated iron oxide nanoclusters involved in the same adsorption experiments in our previous work[25] (in pH 7 water: 21.9 ± 6.8 mg P g^{-1}; in dialysate: 20.7 ± 6.4 mg P g^{-1}). The performance of RSNs@TA for phosphate adsorption was compared with that of similar surfactant-coated iron oxide-based adsorbents, and the adsorption capacity value was comparable to that of the best reported adsorbents. Therefore, the performance of IONPs@PAA and IONPs+PDADMAC is also very competitive compared to the adsorbents reported in the literature.

Therefore, we now consider only IONPs@PAA and IONPs+PDADMAC as potential phosphate adsorbents and compare them. In pH 7 water, the higher adsorption capacity of IONPs+PDADMAC is explained by the "positive surface charge" provided by PDADMAC to the IONPs ($\zeta = 27 \pm 1$ mV, Table 1), which generates attractive electrostatic interactions with phosphate anions (in the form of H$_2$PO$_4^-$/HPO$_4^{2-}$ in pH 7 aqueous media), facilitating their transport to the IO surface until adsorption. On the other hand, despite the fact that IONPs@PAA and IONPs@TA display a "negative surface charge" ($\zeta = -46 \pm 2$ mV and $\zeta = -38 \pm 1$ mV, respectively, Table 1) generating repulsive interactions with phosphate anions, phosphate adsorption is observed even if it is lower. In

dialysate, the significant increase in the adsorption capacity of IONPs@PAA can be explained by the electrolyte-induced charge-screening effect, which decreases the net ζ value of IONPs@PAA to -22 ± 2 mV (Table 1) and thus decreases the repulsive interactions with phosphates. Indeed, the counterions would interact with the PAA chains oriented towards the medium and exhibiting negatively charged carboxylate groups, allowing the phosphates to diffuse towards the IO surface for adsorption. On the other hand, the electrolyte-induced charge screening effect is unfavorable for phosphate adsorption on IONPs+PDADMAC since their positive ζ is slightly decreased to 20 ± 1 mV (Table 1). However, the significant decrease in the IONPs+PDADMAC adsorption capacity does not seem to be fully explained by such a small decrease in zeta potential ($\Delta\zeta = 7$ mV). Furthermore, one may wonder if surfactants are involved in phosphate adsorption. Thus, the presence of phosphates at the surface of IO on IONPs@PAA and IONPs+PDADMAC has been studied and DLS and ELS characterization studies of the surfactant-coated IONPs after phosphate adsorption have been conducted to determine whether their colloidal stability had been altered in each medium.

The presence of phosphates chemically adsorbed on IONPs@PAA and IONPs+PDADMAC has been confirmed by FTIR spectroscopy and X-ray photoelectron spectroscopy (XPS). In IR spectra (Fig. 6a), the characteristic bands of the P–O–Fe bonds have been observed in the 1200–900 cm^{-1} wavenumber range, similar to the work of Daou *et al.*[61] for phosphates adsorbed on

magnetite and to our previous work[25] for phosphates adsorbed on TA-coated nanoclusters. In XPS spectra (Fig. 6b), P 2p peaks are observed at binding energies of 133.1 (IONPs@PAA) and 133.0 eV (IONPs+PDADMAC), close to the value of 133.6 eV reported by Daou *et al.*[61] and other groups in the literature[71,72] and to the value of 133.8 eV obtained in our previous work.[25] All these results confirmed a strong interaction/anchoring of phosphates with the surface of IONPs.

After phosphate adsorption in pH 7 water (Fig. 7a), IONPs@PAA change from a monomodal φ_{hydro} distribution to a bimodal distribution located at 28 nm and 106 nm (by intensity). IONPs@TA retain a monomodal distribution, with an average φ_{hydro} of 145 ± 74 nm (PDI = 0.21). IONPs+PDADMAC also retain a monomodal size distribution, with an average φ_{hydro} decreasing to 226 ± 90 nm (PDI = 0.15). On the other hand, in dialysate (Fig. 7b), the monomodal distribution of IONPs@PAA is preserved, with an average φ_{hydro} of 102 ± 58 nm (PDI = 0.25 nm). However, as discussed above, IONPs@TA sediment, which results in a very high increase in their φ_{hydro} to ≈ 2000 nm. Lastly, IONPs+PDADMAC retain a monomodal distribution, with an increase in their average φ_{hydro} to 903 ± 315 nm (PDI = 0.12) nm. This increase could be related to a possible desorption of PDADMAC from the IO surface during phosphate adsorption, which could also explain the lower adsorption capacity of IONPs+PDADMAC in dialysate compared to pH 7 water (Fig. 5).

These different experiments have enabled us to identify IONPs@PAA and IONPs+PDADMAC as suitable adsorbents with a high phosphate adsorption capacity in pH 7 water and dialysate, fast adsorption of phosphates on their surface, and preservation of their colloidal stability in each solvent after adsorption.

3 Conclusion

In this work, we have designed surfactant-coated IONPs by the coprecipitation method and tested them as potential phosphate adsorbents to be added to the dialysate used in the peritoneal dialysis treatment. The coprecipitation synthesis has been optimized by testing two anionic surfactants, polyacrylic acid (IONPs@PAA) and tannic acid (IONPs@TA), and a cationic one, polydiallyldimethylammonium chloride (IONPs+PDADMAC). These surfactants were chosen for their ability to enhance colloidal stability through electrostatic and/or steric repulsive forces and the coprecipitation method was chosen for its high yield and environmental friendliness. IONPs@PAA and IONPs@TA were obtained in a one-pot synthesis process while IONPs+PDADMAC were obtained by post-synthesis coating of naked IONPs. After the one-pot synthesis, a particle size separation step was necessary and was optimized by using an external magnetic field. All surfactant-coated IONPs were shown to consist of surfactant-coated aggregates of nanograins that were 6–8 nm large for the one-pot synthesis and 9–10 nm large for post-synthesis coating, thus evidencing, as already observed, an effect of the presence of the surfactant during the coprecipitation step.

IONPs@PAA and IONPs@TA have been shown to display a very high colloidal stability over time (at least 3 weeks) in pH 7 water and dialysate displaying high osmolarity and ionic strength with a mean hydrodynamic size in the range of 80–150 nm. IONPs+PDADMAC presented a higher mean hydrodynamic size in both media in the range of ∼350–550 nm and a good colloidal stability over one week suitable for the targeted peritoneal dialysis application. The colloidal stability of IONPs@PAA and IONPs+PDADMAC has been compared with those of commercially available IONPs coated with the same surfactants, and only our IONPs formed stable suspensions in dialysate. Finally, their phosphate adsorption capacities have been studied as a function of time and phosphate concentration: IONPs@TA were shown to flocculate after phosphatation due to the formation of a phosphate-TA complex when IONPs@PAA and IONPs+PDADMAC displayed operative phosphate adsorption in both water and dialysate. Their colloidal stability was quite not affected in dialysate after phosphatation and the presence of phosphates at the surface of IONPs was evidenced.

All these experiments demonstrated that IONPs@PAA and IONPs+PDADMAC are promising phosphate adsorbents for peritoneal dialysis treatment. They will be tested in the future in peritoneal dialysis simulating processes and the possible involvement of surfactants in the phosphate adsorption will also be studied more in depth.

4 Materials and methods

4.1 Materials

Iron(II) chloride tetrahydrate (FeCl$_2$·4H$_2$O, ≥99%, Sigma-Aldrich), iron(III) chloride hexahydrate (FeCl$_3$·6H$_2$O, ≥99%, Sigma-Aldrich), hydrochloric acid (HCl, 37%, CARLO ERBA), tetramethylammonium hydroxide (N(CH$_3$)$_4^+$ OH$^-$, 25 wt% in H$_2$O, Sigma-Aldrich), polyacrylic acid ((C$_3$H$_4$O$_2$)$_n$, ∼2100 Da, Sigma-Aldrich), tannic acid (C$_{76}$H$_{52}$O$_{46}$, Sigma-Aldrich), polydiallyldimethylammonium chloride ((C$_8$H$_{16}$ClN)$_n$, 20 wt% in H$_2$O, Sigma-Aldrich) and orthophosphoric acid (H$_3$PO$_4$, 85+%, Analytical Reagent, for analysis, Fisher Chemical) were used as received.

Ultrapure water was produced using a purification unit PURELAB® flex, ELGA, and PD solution was bicaVera (1.5% GLUCOSE, 1.75 mmol L^{-1} calcium) from Fresenius Medical Care, Germany, with the composition detailed in Table S1.

Commercial PAA- and PDADMAC-coated maghemite nanoparticles were bought from the company "Chemicell". Selected references are "fluidMAG-PAA" (PAA-coated IONPs, approximate φ_{hydro} provided by the supplier: 100 nm) and "fluidMAG-Q" (PDADMAC-coated IONPs, approximate φ_{hydro} provided by the supplier: 200 nm). These references are available in several φ_{hydro} and we have chosen those closest to our own nanoparticles. No tannic acid-coated reference is currently proposed by Chemicell.

4.2 Synthesis conditions of surfactant-coated nanoparticles

4.2.1 Synthesis of naked IONPs. Naked IONPs are synthesized by the coprecipitation method using the protocol of Daou

et al.[30] Briefly, $FeCl_2 \cdot 4H_2O$ (1.0 g) and $FeCl_3 \cdot 6H_2O$ (2.7 g) are added in a HCl solution (12.5 mL, 2 mol^{-1}) and the mixture is homogenized by magnetic stirring for 10 min. Then, the mixture is transferred into a tri-neck round-bottom flask (capacity of 100 mL) and degassed with Ar for 20 min. The mixture is then stirred using a Teflon paddle (250 rpm) and set at 70 °C for 30 min before dropwise adding a $N(CH_3)_4^+$ OH$^-$ solution (26 mL, 0.7 mL min^{-1}) using an Optos Pump 3HI (Eldex). After complete addition (pH $\geq$ 12), the suspension is allowed to cool down to room temperature for 30 min and then washed five times by centrifugation (10 000 rpm, 10 min) with Ar-degassed distilled water. The washed IONPs are suspended in a sufficient volume of Ar-degassed distilled water to prevent aggregation (*i.e.* >100 mL) and the pH is controlled to avoid the isoelectric point of iron oxide (pH$_{IEP} \approx$ 7), *i.e.* pH > 9–10 typically. Finally, the suspension in pH 9–10 Ar-degassed distilled water is placed in an ultrasound bath for 15 min before storage at 4 °C until further characterization or use.

4.2.2 One-pot synthesis of PAA- and TA-coated IONPs. PAA- and TA-coated IONPs are synthesized in one-pot by a coprecipitation method based on the protocol of Daou *et al.*[30] For obtaining IONPs@PAA, $FeCl_2 \cdot 4H_2O$ (1.0 g) and $FeCl_3 \cdot 6H_2O$ (2.7 g) are added in a HCl solution (12.5 mL, 2 mol L^{-1}) and the mixture is homogenized by magnetic stirring for 10 min. For IONPs@TA, only $FeCl_3 \cdot 6H_2O$ (4.1 g) and TA (0.256 g) are added in a HCl solution (12.5 mL, 2 mol L^{-1}) and the mixture is homogenized by magnetic stirring for 1 h. In each case, the mixture is transferred into a tri-neck round-bottom flask (capacity of 100 mL) and then degassed with Ar for 20 min. For obtaining IONPs@PAA, PAA (0.874 g) is added to the mixture after the degassing step. In each case, the mixture is stirred using a Teflon paddle (250 rpm) and heated to 70 °C for 30 min before dropwise adding a $N(CH_3)_4^+$ OH$^-$ solution (26 mL, 0.7 mL min^{-1}) using an Optos Pump 3HI (Eldex). After complete addition (pH $\geq$ 12), the suspension is allowed to cool down at room temperature for 30 min and then diluted in water (400 mL). After natural sedimentation (one week) or magnetic separation (two–four days, see Section 2.4), only the first 300 mL are carefully collected to prevent sampling the largest aggregates and its pH is adjusted to 7 using a HCl solution (2 mol L^{-1}). The resulting suspension is concentrated and washed three times with dH$_2$O in an Amicon Stirred Cell 50 mL (Merck Millipore) and an ultrafiltration disc, PLTK, Ultracel regenerated cellulose, PMNL 10 kD, 44.5 mm (Merck Millipore). Finally, the suspension in pH 7 distilled water is placed in an ultrasound bath for 15 min before being stored at 4 °C until further characterization or use. Typically after a single synthesis and after the complete size separation and washing procedure, ~430 mg (equivalent Fe) of PAA- or TA-coated IONPs are obtained. The percentage yield of small anionic surfactant-coated nanoparticles recovered after sedimentation or magnetic separation is in the range of 28–32%. This current methodology provides enough IONPs to confirm the suitability of this strategy but such a yield could be improved in the future by testing microfluidic approaches.[73,74]

4.2.3 Post-synthesis coating of PDADMAC on naked IONPs. PDADMAC-coated IONPs are obtained by a post-synthesis coating of naked IONPs synthesized using the protocol of Daou *et al.*[30] First, a suspension of naked IONPs in pH 9–10 water (0.75 mL, 20 mg mL^{-1}) is prepared. Separately, a PDADMAC aqueous solution (25 mL, 60 mg L^{-1}) is prepared by dilution of the stock solution (20 wt% in water) with distilled water and is added to the IONP suspension. Thus, the mass ratio PDADMAC/IONP is 100 (here, the ratio is 1500 mg$_{PDADMAC}$/15 mg$_{IO-CP}$ = 100). The mixture is then placed in an ultrasound bath for 15 min before being mechanically stirred overnight. Finally, the suspension is washed five times by centrifugation (10 000 rpm, 10 min) with distilled water. For obtaining enough material for our experiments, sixteen suspensions are typically prepared in parallel resulting in an effectively recovered mass of IONPs+PDADMAC of ~240 mg (*versus* 320 mg theoretically).

4.3 Characterization of the synthesized materials

Transmission electron microscopy (TEM) has been used with a Jeol 2100F transmission electron microscope operating with an acceleration voltage of 200 kV. For sample preparation, suspension drops are deposited on carbon-coated copper grids and samples are observed after solvent evaporation.

X-ray diffraction (XRD) has been performed with a Bruker D8 Discover equipped with a Lynx-Eye detector in the 20–70° (2θ) range with a scan step of 0.03° and a sample rotation of 30 rpm during measurement.

Fourier transform infrared spectroscopy (FTIR) has been performed with a PerkinElmer 100 spectrometer for wavenumbers between 4000 and 400 cm^{-1}. The samples are prepared in pellet form by mixing drops of the material suspension with dry KBr.

Thermogravimetric analysis (TGA) has been performed with a TA Instruments SDT 600 analyzer. The measurement has been performed under an air flow from room temperature to 800 °C at a heating rate of 5 °C min^{-1}. Samples are dried overnight in an oven at 80 °C prior to measurement.

Diffusion light scattering (DLS) and electrophoretic light scattering (ELS) measurements have been performed with Malvern Panalytical Zetasizer Nano ZS equipment.

X-ray Photoelectron Spectroscopy (XPS) experiments are conducted on a VSW-Scientific spectrometer equipped with a twin anode source. XPS spectra were obtained using Al Kα radiation and pass energies of 90 and 22 eV for survey and high-resolution spectra, respectively. All XPS spectra were referenced to the C 1s peak, at 285 eV. Spectral analysis was done with the Casa-XPS software, with the application of Shirley background subtraction and a combination of Gaussian–Lorentzian symmetric and asymmetric line shapes for the peak fitting.

Iron concentration has been measured by NMR ^{1}H-relaxometry[75] using Bruker Minispec 60 equipment working at a Larmor frequency of 60 MHz (1.41 T) at 37 °C.

4.4 Phosphate adsorption in batch mode

Phosphate adsorption kinetics and isotherm experiments are performed similarly to those in our previous work.[25] Briefly, 10 mL of 100 mg P L^{-1} and 600 mg P L^{-1} phosphate solutions in

pH 7 water and in dialysate are added to 10 mL of 2 mg mL^{-1} nanoparticle suspensions in pH 7 water and in dialysate to form 1 mg mL^{-1} nanoparticle suspensions with 50 mg mL^{-1} and 300 mg mL^{-1} of phosphates in pH 7 water and in dialysate. The suspensions are mechanically stirred using an SRT9D roller mixer (Stuart) for 4 hours (adsorption isotherms) and/or 2 hours (adsorption kinetics). The suspensions are then placed in a stirred cell and the surfactant-coated IONPs are separated from the free phosphates by ultrafiltration. The free phosphates are quantified using the VetTest method detailed in our previous work,[25] and the adsorption capacity of the surfactant-coated IONPs is calculated using the following equation:

$$q_E = \frac{(C_O - C_E) \times V}{m} \qquad (1)$$

where C_O and C_E (in mg P L^{-1}) are the initial and equilibrium phosphate concentrations, respectively; V (in L) is the volume of the suspension; and m (in g(Fe$_3$O$_4$)$^{-1}$) is the mass of surfactant-coated IONPs in the suspension.

Author contributions

Philippe Choquet: validation, conceptualization. Anne Carton: methodology, investigation. Jan Niklas Schmidt: visualization, methodology, investigation. Céline Kiefer: methodology, investigation. Ariane Zaloszyc: validation, conceptualization. Théo Lucante: writing – original draft, methodology, investigation, formal analysis. Sylvie Bégin-Colin: visualization, validation, supervision, project administration, methodology, investigation, funding acquisition, conceptualization.

Conflicts of interest

The authors declare that they have no known competing financial interests or personal relationships that could have appeared to influence the work reported in this paper.

Data availability

The authors declare that the data supporting the findings of this study are provided in the article and its supplementary information (SI). Supplementary information is available. See DOI: https://doi.org/10.1039/d6na00103c.

Appendix A

Table detailing the composition of the dialysate used in this work; section detailing the protocol and results for the post-synthesis coating of PAA and TA on naked IONPs in water and containing figures of φ_{hydro} distributions of IONPs at each strategy step, of BET curve of the naked IONPs and a table summarizing the φ_{hydro} by intensity, PDI and ζ values of IONPs at each strategy step; section detailing the magnetic separation process developed for accelerating the recovery of TA- and PAA-coated IONPs with suitable φ_{hydro} distribution and containing figures of φ_{hydro} distributions of IONPs over time during the magnetic separation process and compared to the size

distribution of IONPs recovered after natural sedimentation; XRD pattern of naked and surfactant-coated IONPs; section detailing the characterization of surfactant-coated IONPs by FTIR spectroscopy and containing a table proposing band attribution; section detailing the characterization of surfactant-coated IONPs by TGA; figures of φ_{hydro} distributions of PAA- and TA-coated IONPs at initial time and after 3 weeks in pH 7 water and in dialysate; TEM micrographs of commercial PAA- and TA-coated maghemite nanoparticles; figure of TEM diameter distributions of commercial PAA- and TA-coated maghemite nanoparticles; figure of comparison of φ_{hydro} distributions of our own and commercial IONPs in pH 7 water and dialysate.

Acknowledgements

References

1 J. U. Menon, P. Jadeja, P. Tambe, K. Vu, B. Yuan and K. T. Nguyen, *Theranostics*, 2013, **3**, 152–166.

2 A. Radomska, J. Leszczyszyn and M. W. Radomski, *Adv. Clin. Exp. Med.*, 2016, **25**, 151–162.

3 S.-F. Torabi and Y. Lu, *Curr. Opin. Biotechnol.*, 2014, **28**, 88–95.

4 M. Notarianni, J. Liu, K. Vernon and N. Motta, *Beilstein J. Nanotechnol.*, 2016, **7**, 149–196.

5 J. Wang and H. Gu, *Molecules*, 2015, **20**, 17070–17092.

6 U. S. Ezealigo, B. N. Ezealigo, S. O. Aisida and F. I. Ezema, *JCIS Open*, 2021, **4**, 100027.

7 Y. Q. Meng, Y. N. Shi, Y. P. Zhu, Y. Q. Liu, L. W. Gu, D. D. Liu, A. Ma, F. Xia, Q. Y. Guo, C. C. Xu, J. Z. Zhang, C. Qiu and J. G. Wang, *J. Nanobiotechnol.*, 2024, **22**, 24.

8 C. Blanco-Andujar, A. Walter, G. Cotin, C. Bordeianu, D. Mertz, D. Felder-Flesch and S. Begin-Colin, *Nanomedicine*, 2016, **11**, 1889–1910.

9 M.-S. Martina, J.-P. Fortin, C. Ménager, O. Clément, G. Barratt, C. Grabielle-Madelmont, F. Gazeau, V. Cabuil and S. Lesieur, *J. Am. Chem. Soc.*, 2005, **127**, 10676–10685.

10 Q. Le Trequesser, H. Seznec and M.-H. Delville, *Nanotechnol. Rev.*, 2013, **2**, 125–169.

11 A. Walter, C. Billotey, A. Garofalo, C. Ulhaq-Bouillet, C. Lefèvre, J. Taleb, S. Laurent, L. Vander Elst, R. N. Muller, L. Lartigue, F. Gazeau, D. Felder-Flesch and S. Begin-Colin, *Chem. Mater.*, 2014, **26**, 5252–5264.

12 B. Freis, G. Cotin, F. Perton, D. Mertz, S. Boutry, S. Laurent and S. Begin-Colin, in *Magnetic Nanoparticles in Human Health and Medicine*, eds. C. Caizer and M. Rai, Wiley, 1st edn, 2021, pp. 380–429.

13 V. Nandwana, M. De, S. Chu, M. Jaiswal, M. Rotz, T. J. Meade and V. P. Dravid, in *Nanotechnology-Based Precision Tools for the Detection and Treatment of Cancer*, eds. C. A. Mirkin, T. J. Meade, S. H. Petrosko and A. H. Stegh, Springer International Publishing, Cham, 2015, vol. 166, pp. 51–83.

14 S. Brulé, M. Levy, C. Wilhelm, D. Letourneur, F. Gazeau, C. Ménager and C. Le Visage, *Adv. Mater.*, 2011, **23**, 787–790.

15 J.-P. Fortin, C. Wilhelm, J. Servais, C. Ménager, J.-C. Bacri and F. Gazeau, *J. Am. Chem. Soc.*, 2007, **129**, 2628–2635.

16 R. Di Corato, G. Béalle, J. Kolosnjaj-Tabi, A. Espinosa, O. Clément, A. K. A. Silva, C. Ménager and C. Wilhelm, *ACS Nano*, 2015, **9**, 2904–2916.

17 B. Freis, C. Kiefer, M. de los, A. Ramirez, S. Harlepp, D. Mertz, B. Pichon, C. Iacovita, S. Laurent and S. Begin, *Nanoscale*, 2024, **16**, 20542–20555.

18 D. W. Coyne, S. M. Sprague, M. Vervloet, R. Ramos and K. Kalantar-Zadeh, *J. Nephrol.*, 2022, **35**, 875–888.

19 S. Begin-Colin and D. Felder-Flesch, in *Magnetic Nanoparticles*, CRC Press, 2012, pp. 151–192.

20 S. Laurent, D. Forge, M. Port, A. Roch, C. Robic, L. Vander Elst and R. N. Muller, *Chem. Rev.*, 2008, **108**, 2064–2110.

21 J. Schubert and M. Chanana, *CMC*, 2018, **25**, 4553–4586.

22 A. Walter, A. Garofalo, A. Parat, H. Martinez, D. Felder-Flesch and S. Begin-Colin, *Nanotechnol. Rev.*, 2015, **4**(6), 581–593.

23 W. V. Dorwart and L. Chalmers, *Clin. Chem.*, 1975, **21**, 190–194.

24 F. J. Gennari, *N. Engl. J. Med.*, 1984, **310**, 102–105.

25 T. Lucante, P. Choquet, J. Vaz-Ramos, V. Ball, D. Bégin, C. Leuvrey, V. Papaefthymiou, S. Zafeiratos, A. Zaloszyc and S. Bégin-Colin, *Appl. Surf. Sci.*, 2026, **717**, 164782.

26 T. Lucante, P. Choquet, M. Kretz, A. Zaloszyc and S. Bégin-Colin, *Small Struct.*, 2025, e202500549.

27 S. Prakash and J. Yeom, *Nanofluidics and Microfluidics: Systems and Applications*, William Andrew, Waltham, 1st edn, 2014.

28 A. Rastogi, N. Bhatt, S. Rossetti and J. Beto, *J. Ren. Nutr.*, 2021, **31**, 21–34.

29 R. Massart and V. Cabuil, *J. Chem. Phys.*, 1987, **84**, 967–973.

30 T. J. Daou, G. Pourroy, S. Bégin-Colin, J. M. Grenèche, C. Ulhaq-Bouillet, P. Legaré, P. Bernhardt, C. Leuvrey and G. Rogez, *Chem. Mater.*, 2006, **18**, 4399–4404.

31 S. Lefebure, E. Dubois, V. Cabuil, S. Neveu and R. Massart, *J. Mater. Res.*, 1998, **13**, 2975–2981.

32 CFR 173.73 – Sodium polyacrylate., https://www.ecfr.gov/current/title-21/part-173/section-173.73, (accessed February 26, 2025).

33 CFR 184.1097 – Tannic acid., https://www.ecfr.gov/current/title-21/part-184/section-184.1097, (accessed February 26, 2025).

34 L. M. Sanchez, D. A. Martin, V. A. Alvarez and J. S. Gonzalez, *Colloids Surf., A*, 2018, **543**, 28–37.

35 F. Perton, G. Cotin, C. Kiefer, J.-M. Strub, S. Cianferani, J.-M. Greneche, N. Parizel, B. Heinrich, B. Pichon, D. Mertz and S. Begin-Colin, *Inorg. Chem.*, 2021, **60**, 12445–12456.

36 F. Jones, J. B. Farrow and W. van Bronswijk, *Langmuir*, 1998, **14**, 6512–6517.

37 M. Wiśniewska, T. Urban, E. Grządka, V. I. Zarko and V. M. Gun'ko, *Colloid Polym. Sci.*, 2014, **292**, 699–705.

38 T. Swift, L. Swanson, M. Geoghegan and S. Rimmer, *Soft Matter*, 2016, **12**, 2542–2549.

39 J. L. Weidman, R. A. Mulvenna, B. W. Boudouris and W. A. Phillip, *J. Am. Chem. Soc.*, 2016, **138**, 7030–7039.

40 S. Dultz, R. Mikutta, S. N. M. Kara, S. K. Woche and G. Guggenberger, *Sci. Total Environ.*, 2021, **754**, 142119.

41 C.-L. Lin, C.-F. Lee and W.-Y. Chiu, *J. Colloid Interface Sci.*, 2005, **291**, 411–420.

42 Y. Kuwahara, T. Miyazaki, Y. Shirosaki and M. Kawashita, *RSC Adv.*, 2014, **4**, 23359–23363.

43 K. Hayashi, H. Tomonaga, T. Matsuyama and J. Ida, *J. Appl. Polym. Sci.*, 2022, **139**, 51581.

44 K. Nishio, M. Hasegawa, M. Ikeda, H. Narimatsu, Y. Ogura, N. Gokon, S. Tsubouchi, M. Hatakeyama, M. Abe and H. Handa, *Trans. Mater. Res. Soc. Jpn.*, 2004, **29**(4), 1659.

45 B. Ahmed, A. Syed, K. Ali, A. M. Elgorban, A. Khan, J. Lee and H. A. AL-Shwaiman, *RSC Adv.*, 2021, **11**, 9880–9893.

46 Y. Chiu and Y. Chen, *Anal. Lett.*, 2008, **41**, 260–267.

47 Y.-H. Ma, S.-Y. Wu, T. Wu, Y.-J. Chang, M.-Y. Hua and J.-P. Chen, *Biomaterials*, 2009, **30**, 3343–3351.

48 K. Atacan and M. Özacar, *Colloids Surf., B*, 2015, **128**, 227–236.

49 C. Nadejde, M. Neamtu, V.-D. Hodoroaba, R. J. Schneider, A. Paul, G. Ababei and U. Panne, *J. Nanopart. Res.*, 2015, **17**, 476.

50 M. Bagtash, Y. Yamini, E. Tahmasebi, J. Zolgharnein and Z. Dalirnasab, *Microchim. Acta*, 2016, **183**, 449–456.

51 H. Shagholani and S. M. Ghoreishi, *J. Drug Delivery Sci. Technol.*, 2017, **39**, 88–94.

52 A. R. Biery and D. M. Knauss, *Mater. Today Chem.*, 2022, **26**, 101251.

53 C.-J. Yu, C.-Y. Lin, C.-H. Liu, T.-L. Cheng and W.-L. Tseng, *Biosens. Bioelectron.*, 2010, **26**, 913–917.

54 F. Li, Q. Yang, F. Qiu and Y. Liu, *Polym. Adv. Technol.*, 2016, **27**, 1530–1534.

55 S.-C. Jang, S.-M. Kang, G. Y. Kim, M. Rethinasabapathy, Y. Haldorai, I. Lee, Y.-K. Han, J. C. Renshaw, C. Roh and Y. S. Huh, *Materials*, 2018, **11**, 998.

56 E. Rozhina, A. Danilushkina, F. Akhatova, R. Fakhrullin, A. Rozhin and S. Batasheva, *J. Biotechnol.*, 2021, **325**, 25–34.

57 T. J. Daou, G. Pourroy, J. M. Greneche, A. Bertin, D. Felder-Flesch and S. Begin-Colin, *Dalton Trans.*, 2009, 4442.

58 B. Basly, D. Felder-Flesch, P. Perriat, C. Billotey, J. Taleb, G. Pourroy and S. Begin-Colin, *Chem. Commun.*, 2010, **46**, 985–987.

59 Ferrofluids : Ferromagnetic Particles in Carrier Fluid : Fluidmag, https://www.chemicell.com/products/ferrofluid/ferrofluids.html, (accessed February 26, 2025).

60 R. Massart, *IEEE Trans. Magn.*, 1981, **17**, 1247–1248.

61 T. J. Daou, S. Begin-Colin, J. M. Grenèche, F. Thomas, A. Derory, P. Bernhardt, P. Legaré and G. Pourroy, *Chem. Mater.*, 2007, **19**, 4494–4505.

62 B. Basly, G. Popa, S. Fleutot, B. P. Pichon, A. Garofalo, C. Ghobril, C. Billotey, A. Berniard, P. Bonazza, H. Martinez, D. Felder-Flesch and S. Begin-Colin, *Dalton Trans.*, 2013, **42**, 2146–2157.

63 J. Vaz-Ramos, T. Lucante, J.-M. Greneche, C. Leuvrey, V. Papaefthymiou, S. Zafeiratos, A. Carton, D. Bégin, S. Le Calvé and S. Bégin-Colin, *Colloids Surf., A*, 2024, **689**, 133658.

64 M. Filippousi, M. Angelakeris, M. Katsikini, E. Paloura, I. Efthimiopoulos, Y. Wang, D. Zamboulis and G. Van Tendeloo, *J. Phys. Chem. C*, 2014, **118**, 16209–16217.

65 W. Baaziz, B. P. Pichon, S. Fleutot, Y. Liu, C. Lefevre, J.-M. Greneche, M. Toumi, T. Mhiri and S. Begin-Colin, *J. Phys. Chem. C*, 2014, **118**, 3795–3810.

66 J. Santoyo Salazar, L. Perez, O. de Abril, L. Truong Phuoc, D. Ihiawakrim, M. Vazquez, J.-M. Greneche, S. Begin-Colin and G. Pourroy, *Chem. Mater.*, 2011, **23**, 1379–1386.

67 P. D. Ramirez, C. Lee, R. Fedderwitz, A. R. Clavijo, D. P. P. Barbosa, M. Julliot, J. Vaz-Ramos, D. Begin, S. Le Calvé, A. Zaloszyc, P. Choquet, M. A. G. Soler, D. Mertz,

P. Kofinas, Y. Piao and S. Begin-Colin, *Nanomaterials*, 2023, **13**, 587.

68 O. Gerber, B. P. Pichon, C. Ulhaq, J.-M. Grenèche, C. Lefevre, I. Florea, O. Ersen, D. Begin, S. Lemonnier, E. Barraud and S. Begin-Colin, *J. Phys. Chem. C*, 2015, **119**, 24665–24673.

69 T. Gaudisson, S. K. Sharma, R. Mohamed, B. Sitamtze Youmbi, N. Menguy, F. Calvayrac, M. Seydou and S. Ammar-Merah, *CrystEngComm*, 2021, **23**, 1756–1764.

70 T. J. Daou, J. M. Grenèche, G. Pourroy, S. Buathong, A. Derory, C. Ulhaq-Bouillet, B. Donnio, D. Guillon and S. Begin-Colin, *Chem. Mater.*, 2008, **20**, 5869–5875.

71 W.-H. Lee and J.-O. Kim, *J. Environ. Chem. Eng.*, 2022, **10**, 107103.

72 A. Bunge, C. Leoștean, T. Radu, S. C. Tripon, G. Borodi and R. Turcu, *Magnetochemistry*, 2022, **8**, 79.

73 M. O. Besenhard, A. P. LaGrow, A. Hodzic, M. Kriechbaum, L. Panariello, G. Bais, K. Loizou, S. Damilos, M. Margarida Cruz, N. T. K. Thanh and A. Gavriilidis, *Chem. Eng. J.*, 2020, **399**, 125740.

74 M. O. Besenhard, L. Panariello, C. Kiefer, A. P. LaGrow, L. Storozhuk, F. Perton, S. Begin, D. Mertz, N. T. K. Thanh and A. Gavriilidis, *Nanoscale*, 2021, **13**, 8795–8805.

75 J. Sherwood, K. Lovas and Y. Bao, *AIP Adv.*, 2017, **7**, 056728.